Articles in PresS. J Neurophysiol (February 27, 2008). doi:10.1152/jn.01066.2007

Melanopsin Ganglion Cells Use a Membrane-associated Rhabdomeric Phototransduction Cascade

Dustin M. Graham, Kwoon Y. Wong, Peter Shapiro, Courtney Frederick, Kartik Pattabiraman and David M. Berson*

Department of Neuroscience, Brown University, Box G-LN, Providence, RI 02912, USA.

***Indicates corresponding author**

Abstract

Intrinsically photosensitive retinal ganglion cells (ipRGCs) are photoreceptors of the mammalian eye that drive pupillary responses, synchronization of circadian rhythms, and other reflexive responses to daylight. Melanopsin is the ipRGC photopigment, but the signaling cascade through which this invertebrate-like opsin triggers the photocurrent in these cells is unknown. Here, using patch-clamp recordings from dissociated ipRGCs in culture, we show that a membrane-associated phosphoinositide cascade lies at the heart of the ipRGC phototransduction mechanism, similar to the cascade in rhabdomeric photoreceptors of invertebrate eyes. When ipRGCs were illuminated, melanopsin activated a G protein of the $G_{q/11}$ class, stimulating the effector enzyme phospholipase C (PLC). The presence of these signaling components in ipRGCs was confirmed by single-cell RT-PCR and immunofluorescence. The photoresponse was fully functional in excised inside-out patches of ipRGC membrane, indicating that all core signaling components are within or tightly coupled to the plasma membrane. The striking similarity of phototransduction in ipRGCs and invertebrate rhabdomeric photoreceptors reinforces the emerging view that these cells have a common evolutionary origin.

Introduction

All animal photoreceptors apparently share a common evolutionary origin and belong to one of two parallel lineages that can be traced back at least 600 million years to the last common ancestor of bilaterally symmetric animals (Arendt 2003; Plachetzki et al. 2005). One photoreceptor lineage, now most common in invertebrate eyes, localizes its phototransduction apparatus in microvilli, which

are often tightly packed to form a rhabdomere. The other lineage, of which vertebrate rods and cones are the most familiar members, carries out phototransduction in specialized cilia. Rhabdomeric and ciliary photoreceptors coexist in some extant invertebrates, but vertebrates had been thought to possess only ciliary photoreceptors. However, emerging evidence suggests that a newly discovered photoreceptor type of the mammalian retina, the ipRGC (Berson 2003), might represent a homolog of rhabdomeric photoreceptors (Arendt 2003; Contin et al. 2006; Isoldi et al. 2005; Koyanagi et al. 2005; Melyan et al. 2005; Panda et al. 2005; Provencio et al. 2000; Qiu et al. 2005; Warren et al. 2006). Photoreceptors of the rhabdomeric lineage share a highly conserved phototransduction cascade differing markedly from that in ciliary photoreceptors. Thus, a crucial test of this evolutionary hypothesis is to determine whether the transduction cascade in ipRGCs resembles that of the rhabdomeric lineage.

Phototransduction in ipRGCs begins with light absorption by the photopigment melanopsin (Berson 2003; Hattar et al., 2002; Lucas et al., 2003; Melyan et al. 2005; Provencio et al. 2000; Panda et al. 2005; Qiu et al. 2005), but how this leads to membrane depolarization remains mysterious. The emerging consensus, however, is that phototransduction in these cells may resemble that in rhabdomeric photoreceptors. One reason to suspect this is that melanopsin resembles invertebrate opsins more than vertebrate opsins in its structure (Provencio et al. 2000; Koyanagi et al. 2005) and bistability (Koyanagi et al. 2005; Panda et al. 2005; Melyan et al. 2005; Mure et al. 2007). Furthermore, the depolarizing light responses (Berson 2003) and light-gated conductances of ipRGCs (Warren et al. 2006) also resemble those of rhabdomeric photoreceptors (Hardie and Raghu 2001). In a variety of cell types, native or heterologously expressed melanopsin has been shown or inferred to signal through $G_{q/11}$-class G proteins and the effector enzyme phospholipase C (PLC) (Contin et al. 2006; Isoldi et al. 2005; Koyanagi et al., 2005; Panda et al. 2005; Qiu et al. 2005). This parallels the phototransduction cascade of rhabdomeric photoreceptors (Arendt 2003; Hardie and Raghu 2001) and contrasts with that of rods and cones, which

is based on G_t (transducin) and phosphodiesterase. While the foregoing evidence weighs heavily in favor of a rhabdomeric phototransduction cascade in ipRGCs, there is currently no compelling direct evidence on this point, nor can alternative signaling pathways be conclusively excluded. Melanopsin has been shown in a biochemical assay to activate transducin (Newman et al. 2003) and in a mammalian heterologous expression system to signal through a cascade that includes cyclic nucleotides but not PLC (Melyan et al. 2005). Transducin and cyclic nucleotides are key signaling components in ciliary rather than rhabdomeric photoreceptors. Therefore, a central goal of this study was to test the hypothesis that ipRGC phototransduction is based on a phosphoinositide cascade like that in invertebrate photoreceptors. The results provide the first direct evidence that it is. In whole-cell recordings of ipRGCs in culture, specific blockers of PLC and $G_{q/11}$ class G proteins abolished the light response. Further, by single-cell RT-PCR we confirmed the presence of appropriate G proteins and PLC isozymes (especially, though not exclusively, $G\alpha_{14}$ and PLCβ4).

Phosphoinositide signaling cascades may gate ion channels through either of two second-messenger systems. One involves the diffusible cytoplasmic signaling components IP_3 and Ca^{2+}. The other, involving lipophilic constituents such as DAG and polyunsaturated fatty acids, is localized to the membrane. Both have been implicated in phototransduction in various rhabdomeric receptors. It is unclear, however, which might play a central role in ipRGC phototransduction, and a second goal of this study was thus to address this issue. We show that photocurrents persist in excised inside-out patches of ipRGC plasma membrane, suggesting that all critical signaling components are within the membrane or are tightly coupled to it.

Methods

Retrograde labeling, retinal dissociation and culture

All procedures were conducted in accordance with NIH guidelines and approved by the Institutional Animal Care and Use Committee of Brown University. Adult Sprague-Dawley rats were anesthetized with ketamine [60 mg/kg intraperitoneal (ip)] and medetomidine (0.4 mg/kg ip). Rhodamine labeled fluorescent latex microspheres were deposited unilaterally into the suprachiasmatic nucleus through glass pipettes tilted 10° from vertical (Berson et al. 2002). At least 48 hours after tracer injection, retinas were isolated and briefly inspected by epifluorescence microscopy; only those exhibiting an appropriately sparse distribution of labeled ganglion cells were processed further. Two or three such retinas were pooled and dissociated according to the method of Meyer-Franke et al. (1995). Briefly, retinas were digested in a solution of papain, dissociated by gentle trituration and plated onto 36 poly-L-lysine coated coverslips (BD Biosciences). Cells were incubated in Neurobasal-A supplemented with L-glutamine, B27, brain-derived and ciliary neurotrophic factors, forskolin, and gentamycin at 37°C. Typically, one to five healthy and light responsive ipRGCs could be identified and recorded on each coverslip. These cells were invariably spheroidal and completely devoid of processes.

Recording and photic stimulation

Light responses were recorded in dissociated ipRGCs for up to four days in culture, although most (~90%) were recorded between 12 and 48 hours after dissociation. Single coverslips selected for recording were mounted in a chamber and superfused with carbogenated Ames' medium (2 ml/min; 33°C) as described previously (Wong et al. 2005). Whole cell recordings of retrolabeled isolated ganglion cells were established under visual control using an upright epifluorescence microscope equipped with a water immersion lens (Wong et al. 2005). Pipettes were pulled from thick-walled borosilicate tubing (tip resistances 3 – 7 MΩ) on a Flaming/Brown P-97 puller (Sutter Instruments, Novato, CA). Recordings were made in voltage or current clamp mode with a Multiclamp 700A amplifier (Axon Instruments/Molecular Devices; Sunnyvale, CA). Seal

resistances were 1.5-10 G . Recordings were discarded if series resistance exceeded 30 MΩ at any point during the recording. For voltage-clamp recordings, all cells were held at -74mV. PClamp 9 (Axon Instruments/Molecular Devices) was used for data acquisition. Signals were low-pass filtered at between 200 Hz and 4 kHz, and the sampling frequency was at least 4 times higher than the low-pass filter cutoff. Amplifier was set at a signal gain of 2. Liquid junction potentials (14 mV for the K^+-based internal) were corrected for whole-cell recordings. Internal solutions contained the following (in mM): K-gluconate 120; NaCl 5; KCl 4; HEPES 10; EGTA 2; ATP-Mg 4; GTP-Tris 0.3; phosphocreatine-Tris 7. pH was adjusted to 7.3 with KOH. Photic stimulation was delivered from below and calibrated as described elsewhere (Wong et al. 2005). Briefly, a 100W tungsten-halogen lamp delivered unfiltered broad-band full-field light stimuli. The irradiance of this stimulus, assessed by passing it through narrow band spectral filters, was (in photons·sec^{-1}·cm^{-2}) 4 x 10^{12} at 400nm, 6 x 10^{13} at 500nm and 1 x 10^{14} at 600nm. Photoresponses persisted for >1h in whole-cell recordings.

Excised patch recordings were established by forming a gigohm seal on a dissociated ipRGC soma as above and then withdrawing the pipette from the cell either immediately, without rupturing the patch (for inside-out patches) or within a few minutes of establishing a whole cell recording (for outside-out patches). All n-values described in the Results section represent an excised patch from a different ipRGC. Such patches were always recorded at least 500 µm from the donor cell and typically much farther. For outside-out patch recordings, the internal solution was identical to that used for whole-cell recordings. For inside-out patch recordings, the pipette and bath solutions were symmetrical, and consisted of Ames' medium. Photoresponses persisted for up to 30 min in excised patches. For current clamp recordings from excised patches, we used a gain of 1000 and AC-coupling to accentuate spikes and filter out slow fluctuations in membrane potential. Filter settings and sampling frequencies were the same as stated above for whole-cell recordings.

Pharmacological studies

We introduced individual pharmacological agents in one of three ways. Most lipophilic drugs (U73122, U73343, thapsigargin, OAG) were initially dissolved in DMSO, diluted to their final concentration in Ames' medium, and introduced into the bath by superfusion as previously described (Wong et al. 2007). DMSO did not affect photoresponses when applied alone at the working concentration (≤ 0.1%). Pertussis and cholera toxin were added to the culture medium 24-48 hours before recording. All other drugs were introduced intracellularly by including them in the pipette solution. In most cases, this solution filled the pipette to its tip. However, because the peptides GPAnt-2 and GPAnt-2a impeded seal formation, pipettes were tip-filled with control internal solution before backfilling the rest of the pipette with peptide-containing solution. U73122, GPAnt-2a, GPAnt-2, and thapsigargin were from Tocris, GDPβS from Biomol, and all other agents from Sigma.

Unless otherwise stated, drug effects are expressed as the mean percentage reduction (± standard deviation) relative to the control in the peak light-evoked inward current as measured after ten minutes of drug exposure in darkness. Control currents were measured just before bath application (extracellular agents) or immediately after break-in (intracellular agents). The ten-minute time point was chosen because it was sufficient for the drugs to produce stable steady-state effects but not so long that non-specific reductions in cell health or recording quality would be likely to affect the response. In control recordings, without drug application, although light responses could often be recorded for up to an hour, they gradually became more sluggish and less robust. Statistical significance of drug effects was assessed using a dependent Student's t-test with a one-tailed probability.

Single-cell RT-PCR analysis

Whole-Retinal Library: Whole retinal RNA was used as a positive control for RT-PCR and for primer optimization. Retinas were removed from eye-cups in Hibernate A solution (BrainBits™) and total RNA extracted from whole retinas using an Rneasy Kit column (Qiagen). Total RNA was then primed with oligo$(dT)_{12-18}$ (Invitrogen™), and reverse transcribed using SuperScript III reverse polymerase (Invitrogen™). Incubation times were as follows: 65ºC for 5 minutes, 4ºC for 2 minutes, 50ºC for 60 minutes, 70ºC for 15 minutes.

Cell harvesting and RT-PCR: Primary cultures prepared as above were scanned using the same microscope and chamber as in recording experiments. Single retrolabeled ganglion cells that were well isolated from other cells and debris were aspirated whole into a micropipette, expelled into a PCR tubes containing 20 mM DTT/20 units RNAseOUT (Invitrogen), immediately flash frozen on dry ice and stored at -80ºC overnight. Cells were lysed upon thawing and subsequent incubation at 65ºC during reverse transcription.

Reverse transcription of single cells: Reverse transcription and subsequent in vitro transcription (IVT) were performed using the MessageBooster cDNA synthesis kit for qPCR (Epicentre® Biotechnologies). SuperScript III (Invitrogen™) was used as the reverse trasnscriptase. Approximately 6 µl of cDNA was obtained from each RT reaction. 1 µl of cDNA was used for each PCR reaction to probe for candidate genes. Only cells in which we detected melanopsin transcripts were subjected to further analysis. Bath solution was used as a negative control for RT-PCR contamination. 1 µl of bath solution, approximately the volume of an aspirated cell, was processed in parallel with single-cell material using identical methods. Only GAPDH was detected in this negative control sample.

Primer design: Primers for polymerase chain reaction were designed through Integrated DNA Technologies® using PrimerQuest software. Primers targeted

the 3' portion of the NCBI reference sequence, the last 300 base pairs whenever possible. Whole retinal cDNA was used as a template to test primer specificity and efficiency using real-time PCR. Primers subsequently used to probe for candidate transcripts had amplification efficiencies of greater than 85 % as determined by constructing a standard curve from serial dilutions of the whole-retinal cDNA library. PCR products were run on a gel to confirm that the amplicon was of the predicted size.

Quantitative PCR: PCR amplification was performed using the Platinum SYBR Green qPCR system (Invitrogen™) with an incubation of 50ºC for 2 minutes, an initial denaturation of 95ºC for 2 minutes, followed by 40 cycles of 95ºC for 15 seconds and 60ºC for 1 minute. Melting curve analysis was performed after every run. Final primer concentrations were 0.2 uM. Thermalcycling was performed using Applied Biosystems 7300 Real-Time PCR system. Fluorescent threshold values were set automatically by 7300 System SDS software. The maximum Ct value for detection was set at 40 cycles. Representative amplicons were run on a 2% agarose gel containing 0.5 ug/mL ethidium bromide to confirm amplicon size.

Gene	NCBI ref. seq	Forward Primer	Reverse Primer	Target
GAPDH	NM_017008	AACAGCAACTCCCATTCTTCCACC	CCACCCTGTTGCTGTAGCCATATT	1702-181
GNAq	NM_031036	GAGAGCAAAGCACTCTTTAGAACCATT	TCAGGATGAATTCTCGTGCTGCCT	748-932
GNA11	NM_031033.1	CGTCCATCATGTTCTTGGTGGCAT	TAGGTGATGATTGTGCGGAACAGG	671- 783
GNA14	NM_001013151	CTCTAGATATTGCATTGTGTGTGTCC	GCCACCAGAGCTTTGACAAGGTTT	2517-263
GNA15	NM_053542	ACGAGATCAACCTGTTGTGACACG	ATCTTGGACTTGACTTCCCTTGCC	1261-137
OPN4	NM_138860	AAAGTTCTTTCCTGCGTCTCCTGC	GCTGGCTGTGCATGCAAATAGGTA	1989-216
PLCB1	NM_001077641	GGCAGTGACCCAAATCTCTTCCAT	ACCTCAAGTTGCATCATTGACTCC	4849-500
PLCB2	NM_053478	GAAGTAAAGGAGTCAATGCGGGCT	TGTCTTGTTCACAAGTGGCTCCTG	3500-362
PLCB3	NM_033350	AGGAGTGTCAGGAACAGCGAGAGA	TGCATGACCATTGCTGGCACA	3539-365
PLCB4	NM_024353	TGCAGGTGGTGCATAAAGTGGA	AATCTGACTCCTAGGCTACCGGG	5028-512

GNA15 did not amplify in whole retinal cDNA but did amplify in cDNA prepared from spleen. Although the primers did not span an intron, this was unnecessary

because DNAse would have digested any genomic contamination.

HEK293 cell culture and transfection with PKC biosensor construct

T-cell surface antigen HEK293 cells were grown in Dulbecco's modified Eagle's medium (DMEM; with 4.5 g/L D glucose, L-glutamine, 110 mg/L sodium pyruvate; Invitrogen, Carlsbad, CA) supplemented with 10% fetal bovine serum, and 100 units/ml penicillin, 100 µg/ml streptomycin at 37°C in the presence of 5% CO_2 and exchanged twice weekly. After reaching 75% confluence, cells were transfected with a green fluorescent protein tagged-cys1 domain phosphokinase C fusion protein (GFP-PKC) construct (Oancea et al. 1998) using Lipofectamine 2000 (Invitrogen). Conventional epifluorescence microscopy using blue excitation from a mercury lamp was used to image GFP fluorescence. Each fluorescence image in Fig. 7f and 7g consists of an average of 5 frames captured at 1 frame per second.

Immunofluorescence

Adult rat retinas were isolated, fixed flat for one hour by immersion in 4% phosphate buffered paraformaldehyde, rinsed in 0.1 M phosphate buffer, embedded in agarose and frozen at -20º C in OCT compound. Vertical sections were cut at 16 µm on a cryostat and mounted on Superfrost Plus slides (Fisher Scientific #12-550-15, Pittsburgh, PA). Sections were blocked for one hour in 6% normal donkey serum containing 0.3% Triton-X 100 and incubated for 1-2 days in a mixture of two primary antibodies, anti-melanopsin and anti-PLCβ4. In most cases, the melanopsin antibody was a polyclonal goat antiserum raised against the N-terminus of the rat protein (Santa Cruz catalog #sc269662; 1:50) and the anti-PLCβ4 antibody was a rabbit polyclonal raised against the C terminus of the rat isozyme (Santa Cruz Biotechnology, #SC-404; 1:600). The melanopsin antibody recognizes a single band of appropriate size on Western blots (vendor information) and stains the appropriate RGC population as established in prior publications. The specificity of the anti-PLCβ4 antibody has been documented by its detection of a single band of appropriate molecular weight in Western blots

and the absence of this band in a PLCβ4 knockout (Kano et al. 1998 and data supplied by the vendor). Retinal immunofluorescence obtained with this antibody was abolished in control studies in which the primary antibody was preadsorbed with the immunizing peptide (Santa Cruz catalog #SC-404P). In a few studies, we used a mouse monoclonal anti-PLCβ4 antibody raised against amino acids 752-961 of the C terminus of human PLCβ4 (BD Bioscience Cat #P98520; 1:300) and a rabbit polyclonal antibody against the N-terminus of rat melanopsin (ABR, #PA1-780; 1:1000). Secondary antibodies were a CY3-labeled mouse anti-goat (Jackson; # 205165108); an Alexa-594-labeled donkey anti-mouse (Invitrogen #A21203), and an Alexa-488-labeled donkey anti-rabbit (Molecular Probes A21206).

Calcium imaging of PC12 and HEK293 cells

PC12 cells (kind donation from Dr. Diane Lipscombe's lab) were grown in F-12K Medium (ATCC) supplemented with 2.5% FBS 15% horse serum, and 100 µg/ml streptomycin at 37°C in the presence of 5% CO_2 and exchanged twice weekly. T-cell surface antigen HEK293 cells were grown in Dulbecco's modified Eagle's medium (DMEM; with 4.5 g/L D glucose, L-glutamine, 110 mg/L sodium pyruvate; Invitrogen, Carlsbad, CA) supplemented with 10% fetal bovine serum, and 100 units/ml penicillin, 100 µg/ml streptomycin at 37°C in the presence of 5% CO_2 and exchanged twice weekly. Both HEK293 and PC12 cells were plated separately onto poly-D-lysine coated glass coverslips the night before experiments to enhance cell attachment for imaging. For all imaging experiments cells had their media exchanged with 1ml DMEM containing 5µM of the non-ratiometric calcium indicator Oregon-Green BAPTA-AM (Invitrogen), and were incubated for 30-60 minutes for loading. Cells were imaged on a fixed-stage upright epifluorescence microscope (Nikon E600FN; Melville, NY) equipped with a CCD camera (Dage-MTI). Images were acquired using a frame-grabber card (Scion Corp.) and Scion image software. Frames were acquired at 0.5Hz, and averages of 5 frames were used as data points for plotting change in fluorescence intensity over time. For every cell, we acquired 5 frames

immediately before applying any stimulus and used the average image as the baseline resting fluorescence level. NIH Image J software was used for offline analysis of changes in fluorescence intensity over time. Regions of interest (ROI) were outlined by hand for cell bodies in each field of view for every image, and grey scale profiles were constructed for each pre-stimulus ROI, and each ROI at time points during stimulus application. The peak of each ROI grey scale profile was then used to calculate the percent change in fluorescence intensity at each time point. For all experiments, HEK293 and PC12 cells were continuously superfused with AMES solution to mimic recording conditions of ipRGCs. Carbachol, pertussis toxin, cholera toxin, GTP, 70mM potassium were all dissolved in water. Thapsigargin and CGS21680 were dissolved in DMSO before being diluted in AMES to their working concentration. The working concentration of DMSO was kept at 0.1%. DMSO alone did not affect the cells at this concentration.

Results

Injections of fluorescent retrograde tracer into the suprachiasmatic nucleus but sparing the optic chiasm labeled a few dozen to several hundred ganglion cells scattered across both retinas. After enzymatic dissociation, such cells occurred at very low density in the plated cultures, where they appeared as spheroidal profiles stripped of all processes (Fig. 1, inset). Most of these retrolabeled ganglion cells were ipRGCs, as indicated by robust inward currents evoked by illumination (Fig. 1, black traces). These were indistinguishable from the ipRGC photocurrents recorded in retinal whole-mounts; responses were sluggish, typically peaking at least several seconds after light onset and persisting for up to several minutes after the light was shut off.

Pharmacological evidence for involvement of $G_{q/11}$-class G proteins and PLC

Intracellular application through the patch pipette of the universal G-protein blocker guanosine 5'-[ß-thio]diphosphate (GDPβS; 2mM) completely suppressed

the light response (Fig. 1a, red trace; 98.3% ±3% mean reduction from initial peak photocurrent ± s.d. measured 10 min after break-in; n=4; $p<0.05$ t-test). Thus, melanopsin appears to signal through G proteins in ipRGCs, as expected from the fact that opsins are G–protein-coupled receptors. To determine which G proteins might be responsible, we introduced into ipRGCs the peptide GPAnt-2a, which blocks G proteins of the $G_{q/11}$ class but not those of the $G_{i/o}$ or G_s classes. This eliminated ipRGC photoresponses (Fig. 1b; 95.4%±2.3% reduction; 10 μM ; n=6; $p<0.05$ t-test), whereas a closely related peptide antagonist of $G_{i/o}$ (GPAnt-2; 10 μM) had no effect (5.0%±2.4% reduction; n=4; $p>0.05$ t-test; data not shown). Similarly, robust light responses persisted after prolonged incubation with toxins specifically disrupting signaling through $G_{i/o}$ (pertussis toxin) or G_s (cholera toxin) (250 ng/ml, n=4 for each toxin; Fig.1 c-d). The efficacy of these toxins in blocking their associated G proteins were confirmed in positive control experiments using calcium imaging in PC12 cells (Fig 2).

The effector enzyme for $G_{q/11}$-class G proteins is PLCβ. Bath application of the PLC antagonist U73122 abolished ipRGC light responses during whole-cell recordings (98.4%±0.8% reduction; 5 μM; n=8; $p<0.05$ t-test; Fig. 1e), while the inactive analog U73343 had no effect (5.8%±2.1% reduction; 5 μM; n=3; $p>0.05$ t-test; Fig.1f). The pharmacological manipulations just shown to block photoresponses in dissociated ipRGCs failed to do so in ipRGCs in intact isolated retinas (S. Carlson and D. Berson, unpublished observations). We suspect that this reflects limited access of bath-applied and intracellular agents to all transduction sites in situ, which are widely distributed throughout an extensive arbor of fine dendrites deeply buried within the retina (Berson 2003).

<u>Molecular and immunohistochemical evidence on G protein and PLC expression</u>

The foregoing results implicate $G_{q/11}$ family G proteins and PLCβ in the phototransduction cascade of ipRGCs. To test for the presence of these signaling components in ipRGCs, we conducted single-cell RT-PCR and immunohistochemical studies. Seventeen well-isolated retrolabeled ganglion

cells were harvested from the cultures and each was confirmed to be an ipRGC by detection of melanopsin transcript OPN4. 76% of these cells (13/17) expressed at least one G protein of the $G_{q/11}$ family (Fig. 3). Of these, the most commonly detected was $G\alpha_{14}$ (13/17 cells; 76%), followed by $G\alpha_{q}$ (9/17; 53%) and $G\alpha_{11}$ (5/17; 29%) (Fig. 3). The only other $G_{q/11}$ family G protein in mice is $G\alpha_{15}$. This G protein was undetectable in whole retinal extracts and thus presumably absent in ipRGCs, though we did not test this directly. Positive control experiments confirmed the efficacy of these primers by detection of $G\alpha_{15}$ transcripts in spleen (Wilkie et al., 1991).

We also used single-cell RT-PCR to test for the presence of the four known PLCβ isozymes in ipRGCs. Every ipRGC examined by single-cell RT-PCR tested positive for at least one of these enzymes (Fig. 3). All of them (13/13; 100%) expressed the PLCβ4 isoform, while the remaining three isozymes were expressed in at least a minority of ipRGCs. The most frequently detected of these was PLCβ1 (5/13; 38%) followed by PLCβ3 (4/13; 30%) and PLCβ2 (2/13; 15%) (Fig. 3).

We confirmed the presence of PLCβ4 protein by immunofluorescence microscopy. Vertical sections of rat retina were double labeled using primary antibodies against PLCβ4 and melanopsin (see Methods). The two anti-PLCβ4 antibodies used produced comparable staining patterns, with strong and relatively uniform labeling of the outer and inner plexiform layers as well as the ganglion cell layer (Fig. 4). Somata of ganglion cells stained by the anti-melanopsin antibody were PLCβ4 immunopositive, primarily near their plasma membranes (Fig. 4). Their dendrites were not discernable in the inner plexiform layer presumably because of the uniformly high immunofluorescence in this layer. Other retinal neurons were also PLCβ4 immunopositive, especially horizontal cells, a subset of amacrine cells and some melanopsin immunonegative ganglion cells (Fig. 4). To summarize, these molecular and immunohistochemical data support the implication of the electrophysiological

and pharmacological findings that ipRGCs express members of the $G_{q/11}$ family as well as one or more PLCβ isozymes and that these signaling molecules couple melanopsin to the light-gated channel in ipRGCs.

Evidence for a membrane-associated signaling cascade

Activated PLC hydrolyzes phosphatidylinositol (4,5)-bisphosphate (PIP_2), generating two second messengers: diacylglycerol (DAG), which remains in the membrane; and inositol 1,4,5-trisphosphate (IP_3), which enters the cytosol and binds to IP_3 receptors, triggering Ca^{2+} release from intracellular stores. Our data indicate that the cytosolic branch of this cascade may play a modulatory role, but is apparently not essential for ipRGC phototransduction (Figs. 5-6).

Substantial photoresponses remained >10 min after application of agents disrupting IP_3-mediated Ca^{2+} mobilization (Fig. 5a-d, red traces). Application of thapsigargin to deplete intracellular calcium stores had almost no effect on the amplitude of the light response (11.7%±1.9% reduction after 10 min; 4μM; n=5; $p>0.05$ t-test; Fig. 5b). Positive control experiments, using calcium imaging in HEK293 cells, confirmed that this dose and duration of applied thapsigargin, sufficed to effectively deplete intracellular calcium stores (Fig. 5f). Other drugs that interfere with IP_3-mediated Ca^{2+} mobilization also failed to abolish the light response. We bath-applied heparin to block IP_3 receptors (10.3±7.3% reduction; 1 mg/ml; n=5; $p>0.05$ t-test; Fig. 5a), and also introduced IP_3 into the cell through the pipette to occupy the receptors and blunt the effects of any light-induced IP_3 production (18.3%±1.2% reduction; 100μM; n=4; $p<0.05$ t-test; Fig. 5d). Nor did we observe a current after break-in with pipettes containing IP_3, as would be expected if it were a key second messenger in the phototransduction cascade (Fig. 5e). The above drug effects on response amplitude were assessed 10 min after application. We think it very likely that this was sufficient time for the agents to reach and affect their intended targets. However, even more prolonged exposure of these agents (>30 min) failed to block light responses although gradual response rundown was typical, just as it was in control recordings.

Taken together, the minimal effects of heparin, thapsigargin, and IP_3 suggest that Ca^{2+} mobilization from IP3-sensitive stores is unnecessary for phototransduction. To further test for a role of Ca^{2+} as a second messenger in this cascade, we applied a high concentration of BAPTA (10 mM) through the pipette to chelate intracellular Ca^{2+}. After 10 min, this treatment significantly reduced the light response (70.6±5.4% reduction; n=5; $p<0.05$ t-test; Fig. 5c, red trace), and largely abolished it after 20 min (Fig. 5c, blue trace). Nonetheless given the high mobility of this chelator and the small and compact volume of the recorded cells, one would expect extremely strong and rapid Ca2+ buffering to be in place throughout the cytoplasm within a few minutes. From this perspective, the persistence of substantial photoresponses 10 min after break-in bolsters the earlier evidence against an essential role for IP_3-mediated Ca^{2+} mobilization in ipRGC phototransduction. As discussed below, the more pronounced suppression by BAPTA may reflect its broader-spectrum effects, including its ability to suppress increases in $[Ca^{2+}]_i$ resulting from Ca^{2+} entry or other IP_3-independent mechanisms and to drive intracellular free calcium to such low concentrations that PLC activity is disrupted (Horowitz et al. 2005; Hardie 2005).

By weighing against an essential role for IP_3-mediated calcium mobilization in ipRGC phototransduction, the foregoing evidence lends credence to the alternative hypothesis that PLC activation is coupled to gating of the light-activated channel through a membrane-associated signaling cascade. Other key transduction components, such as melanopsin, G proteins, PIP_2, and the light-gated channels, are also localized to the plasma membrane. We therefore suspected that excised patches of ipRGC membrane might be autonomously photosensitive. This proved to be true. In inside-out patches excised from isolated ipRGCs, light triggered prominent transmembrane currents under voltage clamp (n=3; Fig. 6a) and trains of fast action potentials in current clamp (n=5; Fig. 6b). Outside-out patches of membrane were likewise photosensitive. They exhibited light-induced action potentials that were blocked when TTX was applied through a nearby puffer pipette (n=5; Fig. 6c). They also exhibited

photocurrents under voltage clamp, even when heparin was included in the recording pipette (1 mg/ml) and thapsigargin (4 μM) added to the bath (n=5; Fig. 6d).

Identity of membrane-associated signaling components

Together, the data strongly suggest that neither calcium released from intracellular stores nor any other highly diffusible cytosolic signaling component is essential for phototransduction in ipRGCs. The most straightforward alternative hypothesis is that DAG, the membrane-associated product of PIP_2 hydrolysis, represents the key second messenger in this cascade. However, bath or pipette puffer application of the membrane-permeant and constitutively active DAG analog 1-oleoyl-2-acetyl-sn-glycerol (OAG) failed to induce a current in isolated ipRGCs recorded in whole cell mode (Fig. 7a). Nor did OAG block light responses, even after a 10 min application at a high concentration (100 μM; n=8; Fig.7b). Similar negative results were obtained when another DAG analog, 1,2-Dioctanoyl-sn-glycerol (DOG), was applied in whole-cell recordings and also when OAG or DOG were applied to light-responsive excised patches (data not shown).

In *Drosophila* photoreceptors, which are thought to use a membrane-associated phosphoinositide cascade for phototransduction, DAG analogs likewise fail to induce a current or to block photoresponses (Minke and Parnas 2006), but polyunsaturated fatty acids (PUFAs), which are metabolites of DAG, activate robust currents through light-gated transient receptor potential (TRP) channels (Chyb et al. 1999). We could not reproduce this result in ipRGCs. Exposing ipRGCs to the PUFA arachidonic acid (AA) through a puffer pipette or by fast bath application induced no current (Fig. 7c) nor was there any block of the light response even when applied for 10 minutes at a high concentration (100 μM; n=7; Fig. 7d). Similar negative results were obtained when another PUFA, linolenic acid, was applied during whole-cell recordings and when arachidonic or linolenic acid were applied to light-responsive excised patches (data not shown).

To confirm the efficacy of the DAG analogs and PUFAs used, we conducted positive control experiments in HEK293 cells using a heterologously expressed fluorescent fusion protein that serves as a biosensor for DAG in the plasma membrane (Fig. 7 f-g). We expressed a construct, kindly provided by Dr. Tobias Meyer, that codes for green fluorescent protein fused to the cys1 domain of phosphokinase C. This protein translocates to the cell surface when DAG levels in the plasma membrane increase; this response can be blocked by pre-incubation with arachidonic acid (Oancea et al. 1998). Using this system, we confirmed that the DAG-related agents used above in studies of ipRGCs were pharmacologically effective. As shown in Fig. 7f, OAG (a DAG analog) triggered the expected translocation of the fusion protein in HEK293T cells (Fig. 7f) and pretreatment with arachidonic acid blocked this movement (Fig. 7g). These control studies bolster the significance of the failure of OAG and AA to affect ipRGC phototransduction by ruling out the possibility that they are simply artifacts of poor pharmacological reagents or technique.

The foregoing results suggest that PLC triggers the opening of the light-gated channels by a membrane-associated but DAG-independent mechanism. A plausible candidate for such a mechanism is a direct interaction between PIP_2 and the channel that maintains the channel in a closed state in darkness. Light would stimulate PLC to hydrolyze PIP_2, reducing its abundance and thus releasing the channels into an open state. There is evidence that PIP_2 can either open or close a variety of ion channels, including the light-gated channels in Drosophila (Hardie 2003). A recent groundbreaking paper used sophisticated constructs to show that changes in PIP_2 levels can open channels even when DAG, IP_3 or Ca^{2+} levels are not affected (Suh et al. 2006). Until we develop methods for exploiting such constructs in ipRGCs, a definitive test of this hypothesized signaling mechanism is beyond our means. As a preliminary test of this hypothesis however, we pharmacologically interfered with PIP_2 synthesis using wortmannin. This drug inhibits phosphoinositide 4-kinase (PI4-K), the synthetic enzyme for phosphatidylinositol 4-phosphate (PIP), which is an

essential precursor of PIP_2. According to the hypothesis, wortmannin should slow the termination of the photocurrent at light offset by delaying the restoration of resting levels of PIP_2 and, thus, the closure of the light gated channels. Indeed, when wortmannin was included in the pipette solution (15 μM), response shutoff was dramatically delayed (Fig. 7e). In wortmannin treated cells tested 10 min after break-in, it took more than a minute after light offset for the persistent post-stimulus current to decay to half of peak response amplitude (72 ±12 seconds; mean±s.d.; n=5, Fig. 7e) whereas in control cells such recovery occurred in less than a second (0.8 ± 0.2 seconds; n=5, Fig. 7e). Wortmannin had other effects on phototransduction as well; ipRGCs exposed to the drug exhibited an increase in latency to peak (Fig. 7e red trace), failed to recover back to their pre-stimulus baseline, and were usually unable to generate a second light response (4 out of 5 cells). These data are consistent with the hypothesis that the phototransduction process depletes basal levels of PIP_2, triggering channel opening, and that wortmannin blocks restoration of the closed state by inhibiting PIP_2 re-synthesis. However, these results should be interpreted cautiously because disrupting PI4-K function could affect the transduction cascade in other ways (Kanaho and Suzuki, 2002), and because wortmannin affects a variety of enzymes other than PI4-K (Wipf and Halter, 2005).

Discussion

The central finding of this study is that phototransduction in intrinsically photosensitive retinal ganglion cells is based on a phosphoinositide signaling cascade largely or completely localized to the plasma membrane. It had been well established that melanopsin is the photopigment of ipRGCs, but the downstream signaling cascade in these cells had remained elusive. Melanopsin has been suggested to signal through a phosphoinositide cascade in several native cellular environments (Koyanagi et al. 2005; Isoldi et al. 2005; Contin et al., 2006), and in two heterologous expression systems (Panda et al. 2005; Qiu

et al. 2005). On the other hand, melanopsin, like many G-protein coupled receptors (Hermans 2003), can couple to G proteins of more than one class under some conditions (Melyan et al. 2005; Newman et al. 2003). Thus, the cognate G-protein for melanopsin in ipRGCs, though widely suspected to belong to the G_q family, has never been conclusively established. The present pharmacological data strongly support the hypothesis the one or more G proteins of the G_q family are essential ipRGC phototransduction. Our molecular evidence implicates $G\alpha_{14}$ as the most likely family member to serve this role, since it was detectable in a clear majority of ipRGCs while other family members were never encountered. However, we failed to detect $G\alpha_{14}$ in a minority of sampled ipRGCs. We suspect that this is attributable to the vulnerability of the single-cell RT-PCR method to false negatives (Roeper and Liss 2004), but convergent evidence from complementary methods is needed on this point. The obligate effector enzyme for $G_{q/11}$–class G proteins is PLCβ. The present pharmacological and electrophysiological data confirm the essential role of this enzyme in phototransduction, while the molecular and immunohistochemical findings point to PLCβ4 as the specific isozyme most likely to serve this function.

The reliance of ipRGCs on phosphoinositide signaling for phototransduction distinguishes them from vertebrate rods and cones and underscores their similarity to invertebrate rhabdomeric photoreceptors (Fein and Cavar 2000). The ‘rhabdomeric’ signaling cascade of ipRGCs is congruent with their other invertebrate-like features, including the amino-acid sequence and bistability of their photopigment (melanopsin), the polarity of their light response, and their direct axonal projections to the brain (e.g. Provencio et al. 2000; Melyan et al. 2005; Panda et al. 2005; Koyanagi et al. 2005; Berson 2007). These features support the view that ipRGCs are homologous to invertebrate rhabdomeric photoreceptors, sharing an evolutionary origin in the eyes of a common ancestor of extant invertebrates and vertebrates (Arendt 2003; Plachetzki et al. 2005).

Evidence is emerging for substantial diversity among rhabdomeric photoreceptors in phototransduction mechanisms downstream of PLC, especially in the identity of signaling components and light-gated channels and whether diffusible cytosolic second messengers are required (Hardie and Raghu 2001; Fein and Cavar 2000; Dorlochter and Stieve, 1997). In ipRGCs, the key signaling components downstream of PLCβ appear to be within or closely associated with the plasma membrane. The most compelling evidence for this is the persistence of photosensitivity in isolated inside-out patches of ipRGC membrane. Of course, cytoplasmic constituents tightly linked to the membrane may be retained during patch excision, but readily diffusible constituents such as free Ca^{2+} are presumably precluded from playing a key signaling role under these recording conditions. This implies that the cytosolic branch of the phosphoinositide signaling cascade, mediated by IP_3, is not required for ipRGC phototransduction. This view is reinforced by the fact that light responses persist for hours in whole cell recordings of ipRGCs, including isolated ipRGC somas lacking dendrites, a recording configuration in which the dialysis of diffusible cell constituents is presumably very intensive. Further, such responses persist when IP_3 receptors are blocked or flooded with their ligand, calcium stores are depleted, or (at least over the short term) when intracellular calcium is chelated (Fig.4). Highly diffusible cytosolic components thus appear unnecessary for basic phototransduction in ipRGCs, though they undoubtedly play important modulatory roles under physiological conditions, such as adaptation, gain control and response termination.

The data of Fig. 5c may suggest to some readers that Ca^{2+} could serve as an essential second messenger in ipRGC phototransduction. When intracellular free calcium in ipRGCs was thoroughly chelated by BAPTA, the light response was significantly attenuated after 10 min and largely abolished after 20 min. It is important to recognize, however, that chelating all intracellular free calcium is a drastic manipulation that affects Ca^{2+} derived from all sources. This can be expected to alter countless proteins and physiological processes that depend on

some minimal level of basal free Ca^{2+}. It is of particular relevance that PLC activity is Ca^{2+}–dependent (Horowitz et al. 2005; Hardie 2005), because our data identify this as the essential effector enzyme for ipRGC phototransduction. Further, if Ca^{2+} served as an essential intracellular second messenger for the core melanopsin signaling cascade, one would expect the photoresponse to be abolished within seconds as BAPTA, a fast Ca^{2+} chelator, diffuses throughout the cytosol of these small, compact cultured cells. Because the complete loss of the response takes orders of magnitude longer than this, the evidence suggests that Ca^{2+} seems to play a permissive, and perhaps modulatory role in ipRGC phototransduction, not an instructive one.

A very recent study by Peirson et al (2007) may also be viewed as arguing against a purely membrane-associated phototransduction cascade in ipRGCs. They provided intriguing evidence that a particular isoform of protein kinase C (PKCzeta) may play an important role in the generation of ipRGC photoresponses. They showed that this enzyme is expressed in ipRGCs and that its transcription in the retina is upregulated by light, ostensibly through a melanopsin-dependent process. They further showed that PKCzeta knockout mice exhibit a behavioral phenotype mimicking that of melanopsin knockout animals. At this point, it is unclear whether the behavioral phenotype in PKCzeta knockouts results from disruption of ipRGC phototransduction per se, since it could also be explained by defects in axon outgrowth, pathfinding, synaptogenesis, or presynaptic release. If these animals do indeed have a phototransduction defect, it would still be uncertain that PKCzeta plays a crucial signaling (instructive) role in the cascade. It might, instead, play a permissive role, for example by enabling the proper development or maintenance of the transduction machinery. Even if a key signaling role for PKCzeta in the phototransduction cascade can be established, this need not conflict with the present evidence for a membrane-associated cascade. Though PKC isozymes are often found within the cytosol, they can be recruited to the membrane. In

fact, Peirson et al (2007) localized PKCzeta to the ipRGC plasma membrane. Thus, it could have been retained during our excision of isolated patches.

The phototransduction cascade in ipRGCs bears a particularly strong resemblance to that in Drosophila photoreceptors (Hardie and Raghu 2001) in that it appears membrane-associated and does not require IP_3. The similarities are extended by the present evidence implicating PLCβ4 as the most likely effector enzyme in ipRGCs because this is the mammalian PLCβ isozyme most closely related to the PLC-norpA effector enzyme in Drosophila photoreceptors (Lee et al. 1993). The similarities between ipRGCs and Drosophila photoreceptors may extend even to the general form of the light-gated channel. In ipRGCs, available evidence has raised the possibility that photocurrents may be carried by members of the canonical subfamily of transient receptor potential (TRPC) channels (Warren et al. 2006; Sekaran et al. 2007, Berson 2007), the closest mammalian homologs of the light-gated TRP and TRPL channels in Drosophila photoreceptors. The present evidence is in keeping with this view because both ipRGC light-operated channels and TRPC channels can be gated by G-protein-stimulated phosphoinositide signaling, at least in part by a membrane-delimited pathway (Chyb et al 1999). However, our data may also pose a problem for the hypothesis that TRPCs are the light-gated channel in ipRGCs. DAG analogs and metabolites, which activate both Drosophila TRP channels and many mammalian TRPC channels, failed to induce a current in ipRGCs or to occlude the light-evoked current. It seems safe to say that uncertainty about the identity of the light gated channels in ipRGCs remains the most glaring gap in our understanding of phototransduction mechanisms in these neurons.

References

Arendt D. Evolution of eyes and photoreceptor cell types. Int J Dev Biol 47: 563-571, 2003.

Berson DM, Dunn FA, Takao M. Phototransduction by retinal ganglion cells that set the circadian clock. Science 295: 1070-1073, 2002.

Berson DM. Strange vision: ganglion cells as circadian photoreceptors. Trends Neurosci 26: 314-320, 2003.

Berson DM. Phototransduction in ganglion-cell photoreceptors. Pflugers Arch. 454: 849-855, 2007.

Chyb S, Raghu P, Hardie RC. Polyunsaturated fatty acids activate the Drosophila light-sensitive channels TRP and TRPL. Nature 397 : 255-259, 1999.

Contin MA, Verra DM, Guido ME. An invertebrate-like phototransduction cascade mediates light detection in the chicken retinal ganglion cells. Faseb J 20: 2648-2650, 2006.

Dorlöchter M, Stieve H. The Limulus ventral photoreceptor: light response and the role of calcium in a classic preparation. Prog Neurobiol. 53: 451-515, 1997.

Fein A, Cavar S. Divergent mechanisms for phototransduction of invertebrate microvillar photoreceptors. Vis Neurosci 17: 911-917, 2000.

Guarnieri S, Fano G, Rathbone MP, Mariggio MA . Cooperation in signal transduction of extracellular guanosine 5' triphosphate and nerve growth factor in neuronal differentiation of PC12 cells. Neuroscience 128: 697-712, 2004.

Hardie RC, Raghu P. Visual transduction in Drosophila. Nature 413: 186-193, 2001.

Hardie RC. TRP channels in Drosophila photoreceptors: the lipid connection. Cell Calcium 33: 385-393, 2003.

Hardie RC. Inhibition of phospholipase C activity in Drosophila photoreceptors by 1,2-bis(2-aminophenoxy)ethane N,N,N',N'-tetraacetic acid (BAPTA) and di-bromo BAPTA. Cell Calcium 38: 547-556, 2005

Hattar S, Liao HW, Takao M, Berson DM, Yau KW. Melanopsin-containing retinal ganglion cells: architecture, projections, and intrinsic photosensitivity. Science 295: 1065-1070, 2002.

Hermans E. Biochemical and pharmacological control of the multiplicity of coupling at G-protein-coupled receptors. Pharmacol Ther 99: 25-44, 2003.

Horowitz LF, Hirdes W, Suh BC, Hilgemann DW, Mackie K, Hille B. Phospholipase C in living cells: Activation, inhibition, Ca^{2+} requirment, and regulation of M current. J. Gen. Physiology 126: 243-262, 2005.

Isoldi MC, Rollag MD, Castrucci AM, Provencio I Rhabdomeric phototransduction initiated by the vertebrate photopigment melanopsin. Proc Natl Acad Sci U S A 102: 1217-1221, 2005.

Kanaho Y, Suzuki T. Phosphoinositide kinases as enzymes that produce versatile signaling lipids, phosphoinositides. J Biochem (Tokyo). 131: 503-509, 2002.

Kano M, Hashimoto K, Watanabe M, Kurihara H, Offermanns S, Jiang H, Wu Y, Jun K, Shin HS, Inoue Y, Simon MI, Wu D. Phospholipase cbeta4 is specifically involved in climbing fiber synapse elimination in the developing cerebellum. Proc Natl Acad Sci U S A 26:15724-15729, 1998.

Koyanagi M, Kubokawa K, Tsukamoto H, Shichida Y, Terakita A. Cephalochordate melanopsin: evolutionary linkage between invertebrate visual cells and vertebrate photosensitive retinal ganglion cells. Curr Biol 15: 1065-1069, 2005.

Lee CW, Park DJ, Lee KH, Kim CG, Rhee SG. Purification, molecular cloning, and sequencing of phospholipase C-beta 4. J Biol Chem 268: 21318-21327, 1993.

Liss B, Roeper J. Correlating function and gene expression of individual basal ganglia neurons. Trends Neurosci 27:475-81, 2004.

Lucas RJ, Hattar S, Takao M, Berson DM, Foster RG, Yau KW. Diminished pupillary light reflex at high irradiances in melanopsin-knockout mice. Science 299: 245-247, 2003.

Luo D, Broad LM, Bird GJ, Putney JW. Signaling pathway underlying muscarinic receptor-induced Ca2+ oscillation in HEK293 cells, J. Biol. Chem. 276: 5613–5621, 2001

Melyan Z, Tarttelin EE, Bellingham J, Lucas RJ, Hankins MW. Addition of human melanopsin renders mammalian cells photoresponsive. Nature 433: 741-745, 2005.

Meyer-Franke A, Kaplan MR, Pfrieger FW, Barres BA. Characterization of the signaling interactions that promote the survival and growth of developing retinal ganglion cells in culture. Neuron 15: 805-819, 1995.

Minke B, Parnas M. Insights on TRP channels from in vivo studies in Drosophila. Annu. Rev. Physiol 68; 649-684, 2006.

Mure LS, Rieux C, Hattar S, Cooper HM. Melanopsin-dependent nonvisual responses: evidence for photopigment bistability in vivo. J Biol Rhythms 22: 411-424, 2007.

Newman LA, Walker MT, Brown RL, Cronin TW, Robinson PR. Melanopsin forms a functional short-wavelength photopigment. Biochemistry 42: 12734-12738, 2003

Oancea E, Teruel MN, Quest AF, Meyer T. Green fluorescent protein (GFP)-tagged cysteine-rich domains from protein kinase C as fluorescent indicators for diacylglycerol signaling in living cells. J Cell Biol 140: 485-498, 1998.

Panda S, Nayak SK, Campo B, Walker JR, Hogenesch JB, Jegla T. Illumination of the melanopsin signaling pathway. Science 307: 600-604, 2005.

Park TJ, Chung S, Han MK, Kim UH, Kim KT. Inhibition of voltage-sensitive calcium channels by the A_{2A} adenosine receptor in PC12 cells. J. Neurochem. 71: 1251-1260, 1998.

Plachetzki DC, Serb JM, Oakley TH. New insights into the evolutionary history of photoreceptor cells. Trends Ecol Evol 20: 465-467, 2005.

Provencio I, Rodriguez IR, Jiang G, Hayes WP, Moreira EF, Rollag MD. A novel human opsin in the inner retina. J Neurosci 20: 600-605, 2000.

Qiu X, Kumbalasiri T, Carlson SM, Wong KY, Krishna V, Provencio I, Berson DM. Induction of photosensitivity by heterologous expression of melanopsin. Nature 433: 745-749, 2005.

Sekaran S, Lall GS, Ralphs KL, Wolstenholme AJ, Lucas RJ, Foster RG, Hankins MW. 2-Aminoethoxydiphenylborane is an acute inhibitor of directly photosensitive retinal ganglion cell activity in vitro and in vivo. J Neurosci. 27:3981-3986. 2007

Suh BC, Inoue T, Meyer T, Hille B. Rapid chemically induced changes of PtdIns(4,5)P2 gate KCNQ ion channels. Science 314: 1454-1457, 2006.

Warren EJ, Allen CN, Brown RL, Robinson DW. The light-activated signaling pathway in SCN-projecting rat retinal ganglion cells. Eur J Neurosci 23: 2477-2487, 2006.

Wipf P, Halter RJ. Chemistry and biology of wortmannin. Org Biomol Chem. 3:2053-2061, 2005.

Wong KY, Dunn FA, Berson DM. Photoreceptor adaptation in intrinsically photosensitive retinal ganglion cells. Neuron 48: 1001-1010, 2005.

Wong KY, Dunn FA, Graham DM, Berson DM. Synatpic influences on rat ganglion-cell photoreceptors. J Physiol. 582: 279-296, 2007.

Acknowledgements We thank Andy Hartwick for advice on retinal dissociation, Anita Zimmerman, Julie Kauer, Barry Connors and David Clapham for helpful discussions, Dianne Boghossian for technical help, Kiersten Derby and Rie Masui for preliminary work on G-protein mRNA, and Tobias Meyer for the eGFP-PKCγC1$_2$ construct. This work was supported by separate Ruth L. Kirschstein National Research Service Awards to D.M.G. and K.Y.W, and by National Institutes of Health grants R01 EY12793 and EY17137 to D.M.B.

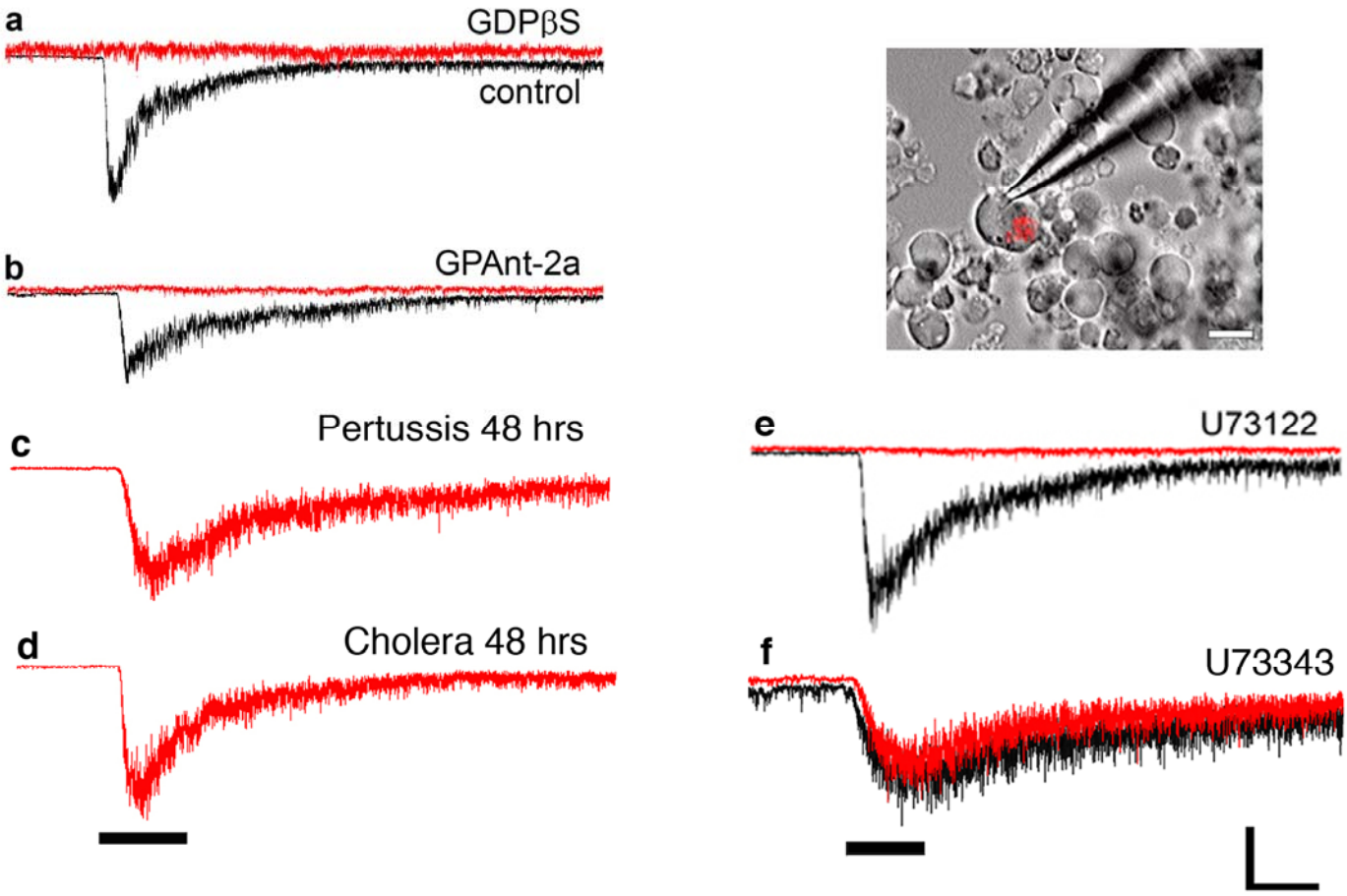

FIGURE 1. Whole-cell voltage-clamp recordings of photocurrents in isolated ipRGCs under control conditions (black traces) and in presence of agents blocking various phototransduction components (red traces). Horizontal black bars represent light stimulus for all traces above them. Photocurrents were abolished by antagonists of G-protein-mediated phosphoinositide signaling, including **(a)** a non-specific G-protein antagonist, **(b)** a specific blocker of $G_{q/11}$-class G proteins, and **(e)** an inhibitor of the effector enzyme PLC. Pre-incubation (48 hours) with toxins disrupting function of $G_{i/o}$ G proteins **(c)** or G_s G proteins **(d)** did not block light responses. **(f)** The inactive U73122 analog (U73343) had no effect on photocurrents. Inset: overlaid Nomarski and fluorescence images showing recording of isolated, retrolabeled ipRGC; scale = 10 μm. For bath-applied agents **(e-f)**, traces show currents before and 10 min after bath application. For internally applied agents (**a-b**), traces show current immediately after break-in (black) and 10 min after break-in (red). **(c-d**) agents were included in culture media for 48 hours prior to recording, and cells were recorded with perfused Ames' solution. Calibration: 5 sec; 40 pA for all traces. Basal currents (-5 to -40 pA) have been normalized.

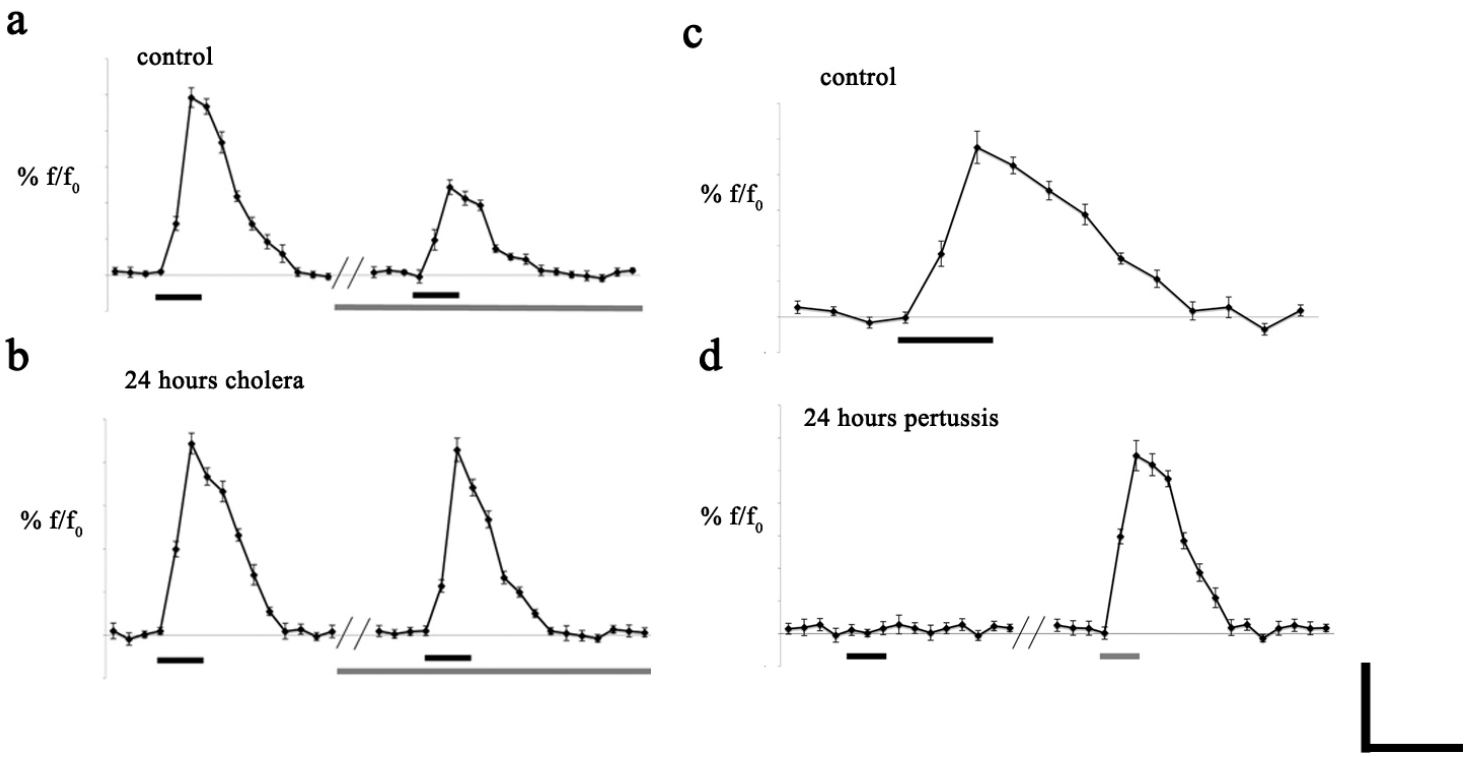

Figure 2. Positive controls for pertussis and cholera toxins: **(a-b)** PC12 cells were loaded with the calcium indicator Oregon-Green BAPTA-AM and their responses to 70mM high potassium external solution (black bar) was monitored with fluorescent imaging. **a)** Control PC12 cells were treated with 10 nM CGS21680 (grey bar), an A2A adenosine receptor-specific agonist known to inhibit voltage-gated calcium channels through a cholera toxin sensitive pathway in PC12 cells (Park et al. 1998). PC12 cells showed an average of ~50% reduction in response to high potassium under these conditions (n=12; error bars indicate standard deviation). **b)** PC12 cells pre-incubated for 24 hours in 500nM cholera toxin did not show any such decrease in response to 70mM potassium (black bar) after bath applied 10nM CGS21680 (grey bar) (n=14; error bars indicate standard deviation). **(c-d)** PC12 cells were loaded with the calcium indicator Oregon-Green BAPTA-AM and their responses to 100μM bath applied GTP (black bar) was monitored with fluorescent imaging. GTP has been shown to transiently increase intracellular calcium concentration through a pertussis toxin sensitive pathway, involving endogenous L-type voltage-gated calcium channels and intracellular calcium stores (Guarnieri et al. 2004). **c)** Control cells showed a strong increase in calcium concentration when GTP was quickly perfused into the bath (n=12; error bars indicate standard deviation). **d)** PC12 cells pre-incubated for 24 hours in 500nM pertussis toxin however, showed no response to bath applied GTP (bottom panel, black bar), but were still responsive to 70mM high potassium external solution (grey bar) indicating the pertussis toxin effect was specific and not lethal to the cells (n=10; error bars indicate standard deviation).

Gap in recordings **(a-d)** between angled lines represents 10 minutes. Calibration: **(a,b,d)** 60 sec; 5% **(c)** 30 sec; 5%.

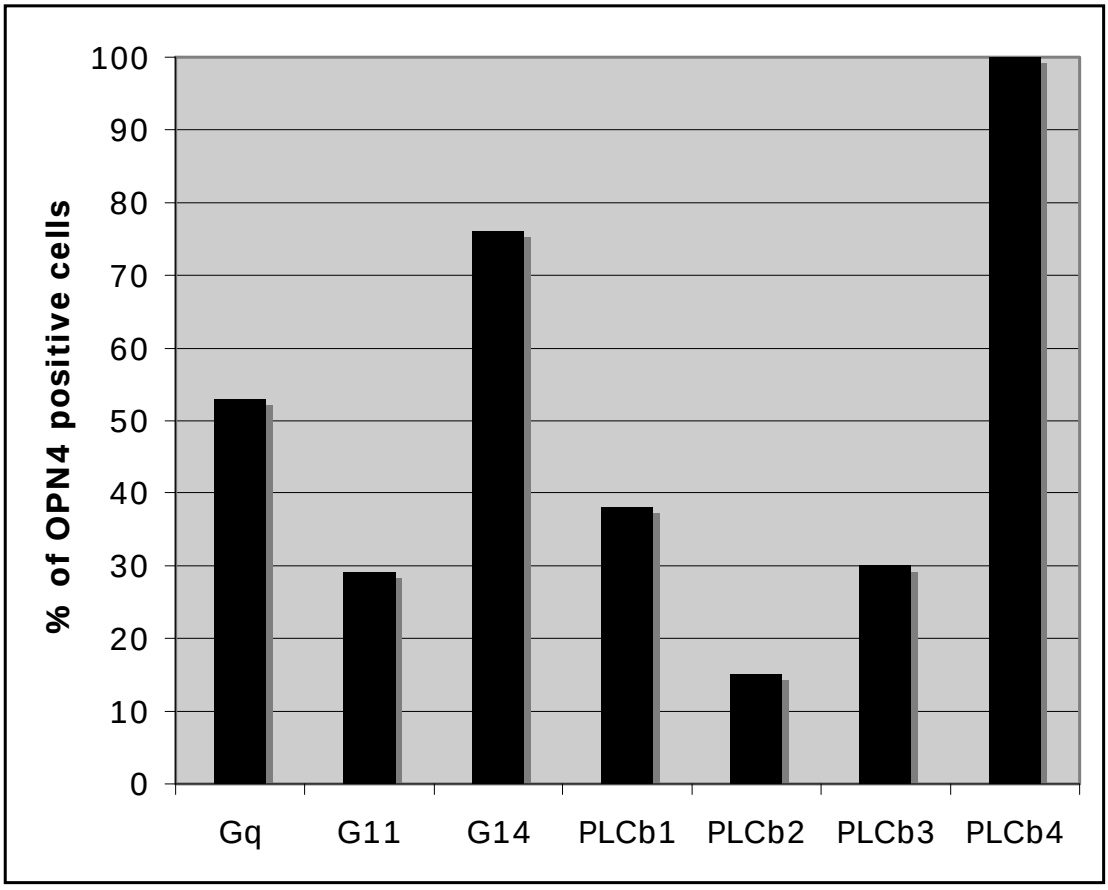

Figure 3. Single-cell RT-PCR evidence of the expression of $G_{q/11}$ subunits and PLCβ isozymes in melanopsin ganglion cells (identified by SCN retrolabeling and detection of melanopsin [OPN4] transcripts)

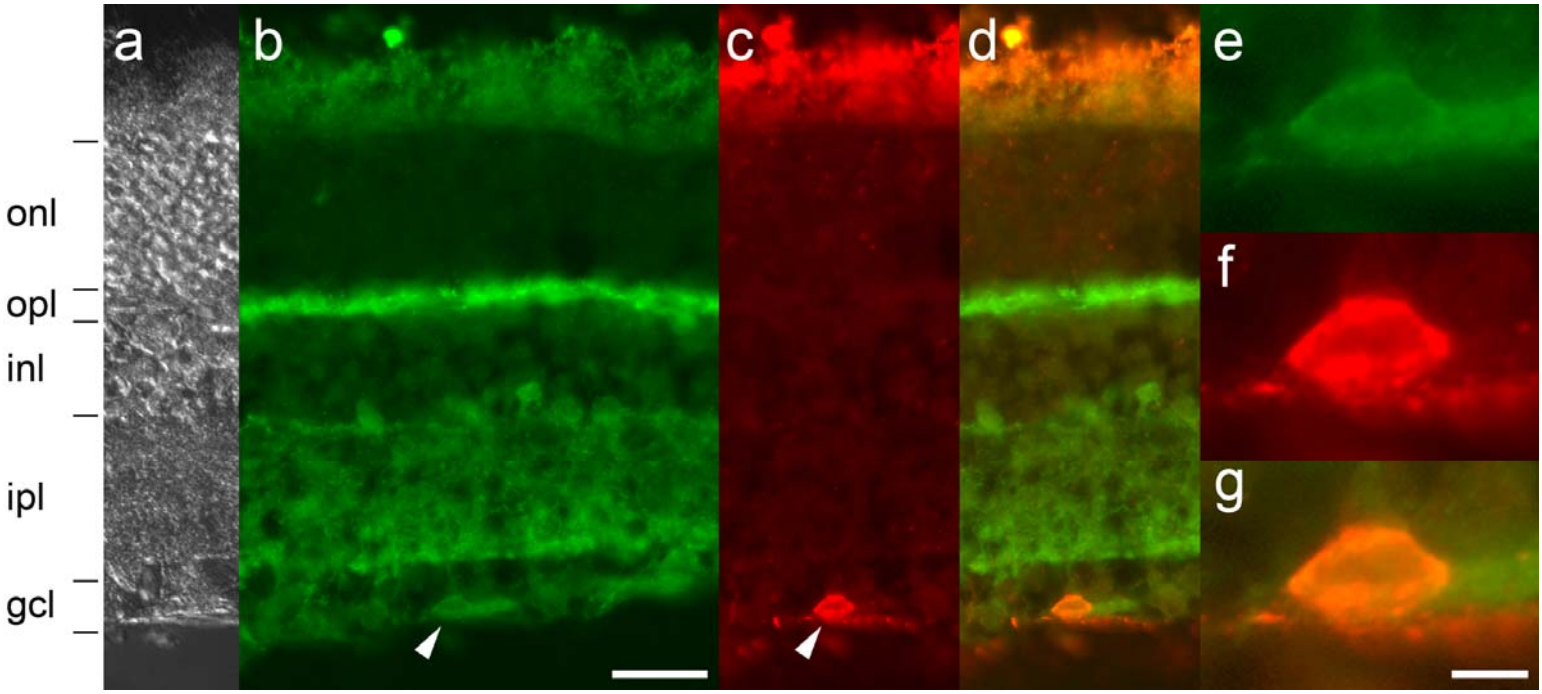

Figure 4. Immunohistochemical evidence for colocalization of PLCβ4 and melanopsin in ipRGCs. **a - d**: multiple views of the same vertical section of rat retina illustrating **a**) cell layers as viewed in Nomarski optics; **b**) PLCβ4-like immunofluorescence (green; antibody: #sc269662); **c**) melanopsin-like immunoreactivity (red; antibody: #SC-404); and **d**) merge of b and c. Arrowheads mark a melanopsin-positive ipRGC. **e - f**: enlarged views of the melanopsin positive cell in b-d. Scale bar in b equals 50 μm for panels a-d; scale bar in g equals 10 μm for e-g.

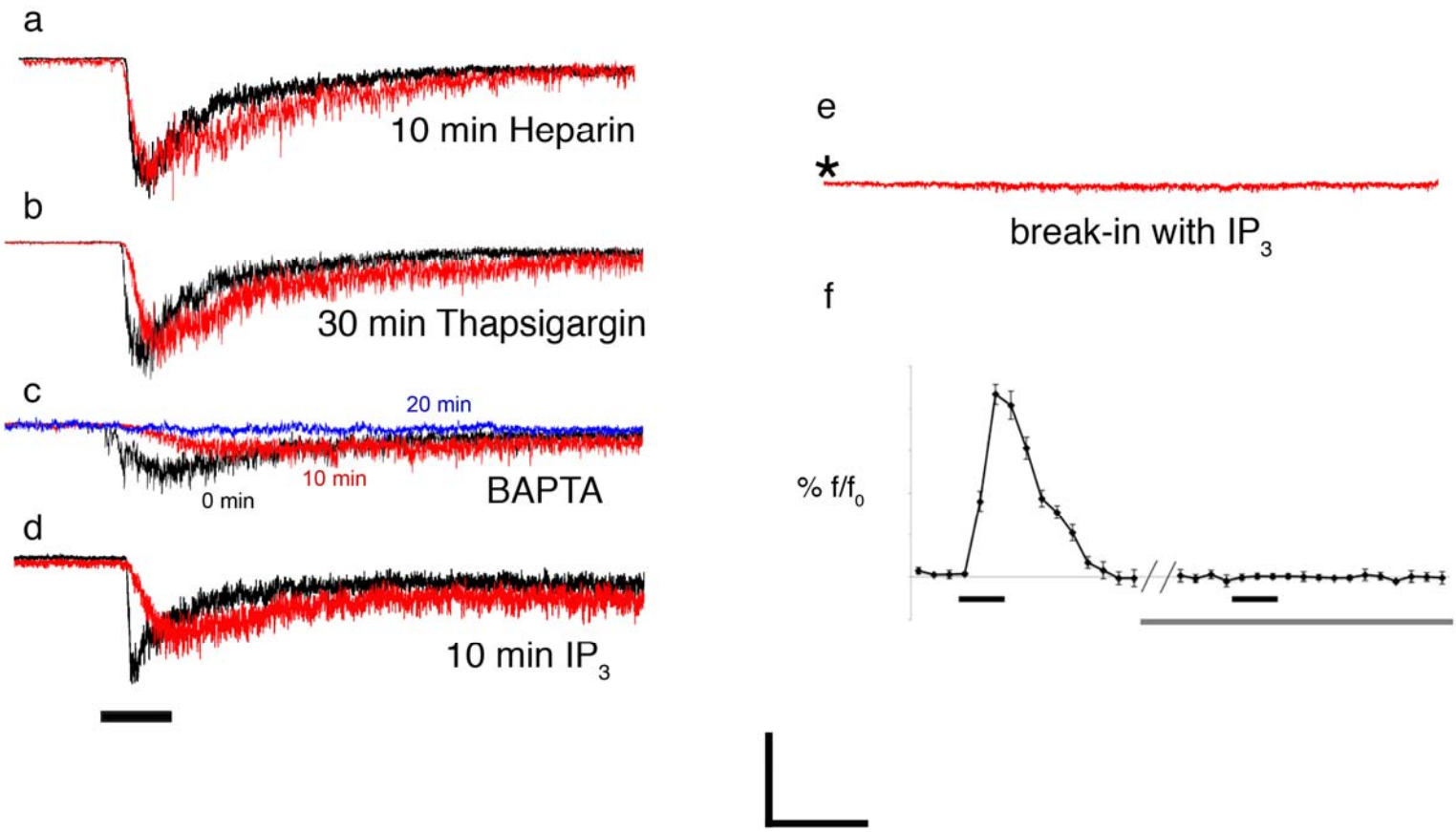

Figure 5. Whole-cell voltage-clamp recordings from melanopsin ganglion cells showing effects on photocurrent of agents altering IP_3-mediated Ca^{2+} mobilization including **(a)** a blocker of IP_3 receptors, **(b)** an agent depleting intracellular Ca^{2+} stores, **(c)** a chelator of intracellular Ca^{2+}, and **(d)** the native ligand of IP_3 receptors. Black bar represents light stimulus for all traces above it. **(e)** Example trace of an ipRGC recorded with IP_3 in the pipette immediately following break-in (denoted by asterisk). Note the lack of response. **(f)** Positive control for thapsigargin: HEK293 cells were loaded with the calcium indicator Oregon-Green BAPTA-AM and their responses to bath applied 100μM carbachol (black bar), a muscarinic receptor agonist that causes release of calcium from intracellular stores (Luo et al. 2001.), were monitored by fluorescent imaging. Ten-minute incubation in 4μM thapsigargin completely abolished the response to carbachol indicating that the calcium stores had been completely depleted (n=10; error bars indicate standard deviation). Gap in recording between angled lines indicates 10 minutes. Calibration: **(a-e)** 10 sec; 100 pA; **(f)** 60 sec; 5%.

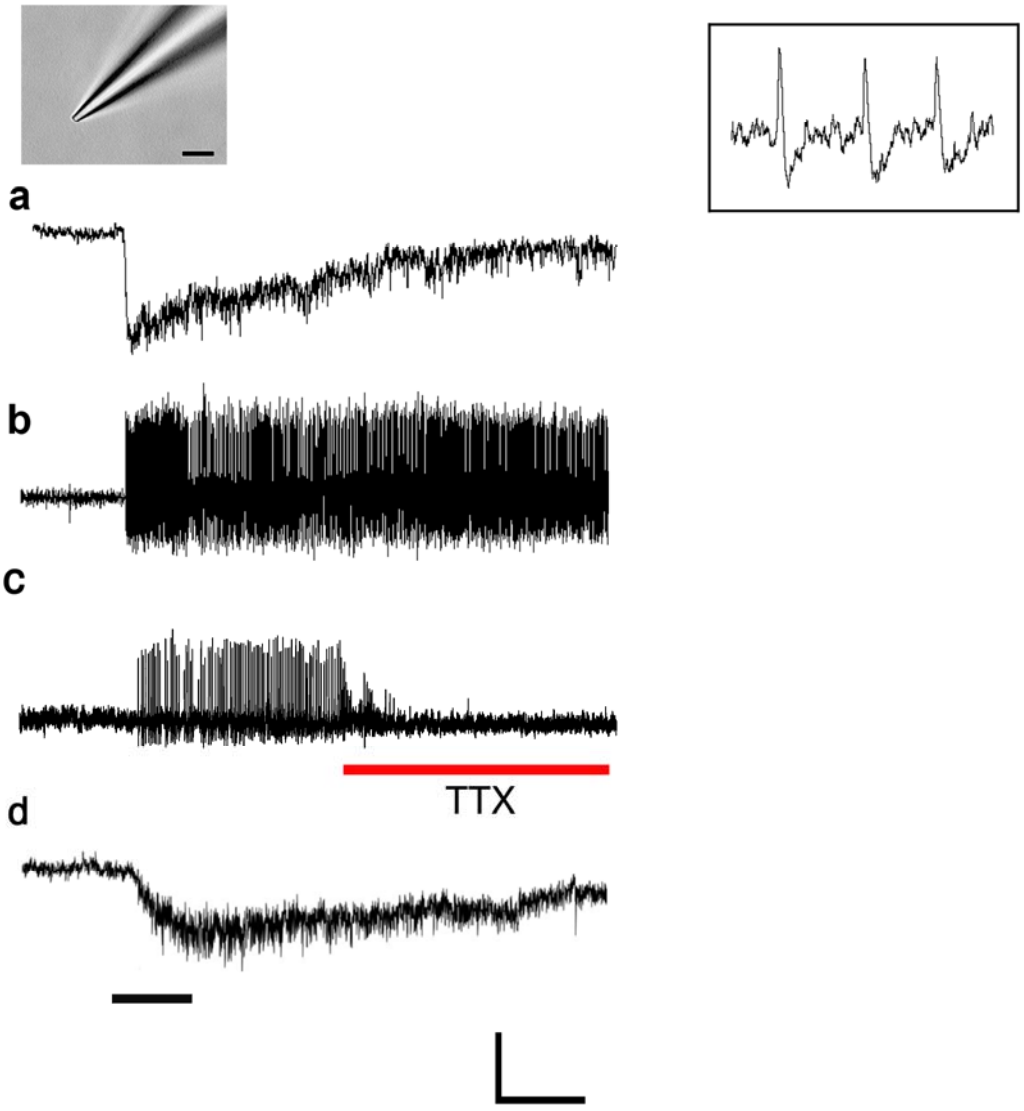

Figure 6. Photoresponses from excised patches of ipRGC membrane. **(a)** Inward photocurrent recorded under voltage clamp (+74mV) from the inside-out patch illustrated in left inset (scale: 10 μm). **(b)** Light-evoked voltage response from inside-out patch recorded in AC coupled current clamp mode. **(c)** Blockade by tetrodotoxin of light-evoked spikes from an outside-out patch of ipRGC membrane. **(d)** Photocurrent from an outside-out patch recorded under voltage clamp (-74mV) with heparin in pipette and thapsigargin in bath. **Right inset**: Extended x-axis view of spikes from an outside-out patch of ipRGC membrane responding to light. Calibration: **(a, d)** 6s and 10 pA **(b-c)** 6s and 0.2 mV **(right inset)** 50ms and 0.2 mV. Black bar represents light stimulus for all traces above it.

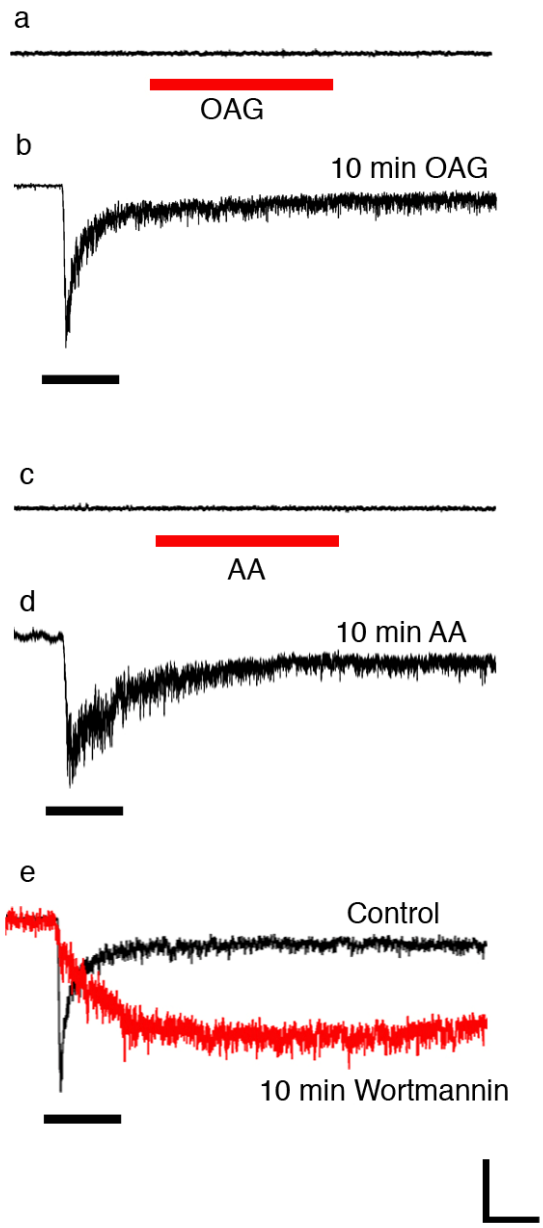

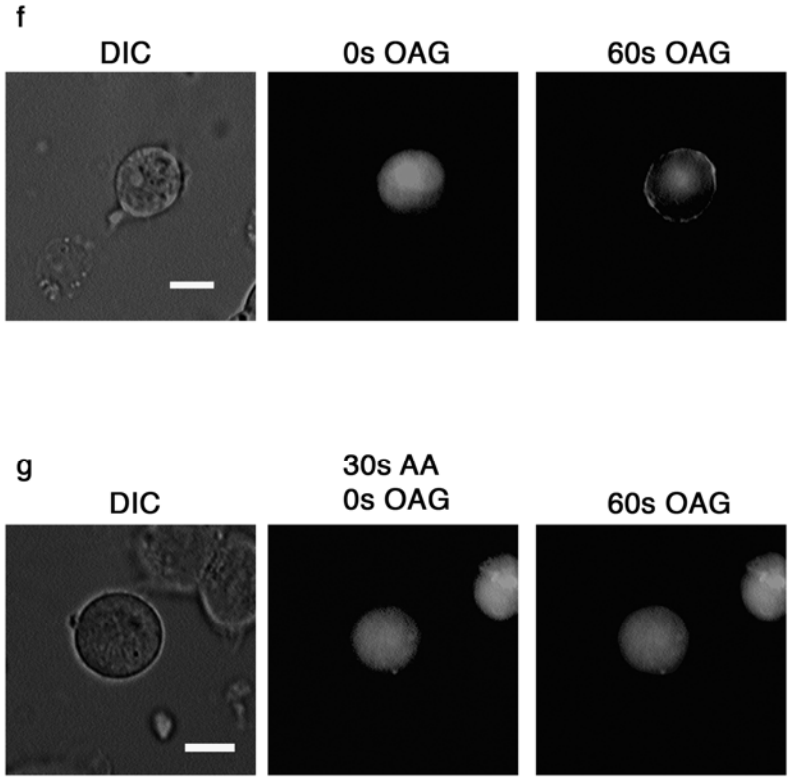

Figure 7. Evidence concerning possible gating of the light-activated channel of ipRGCs by DAG, polyunsaturated fatty acids (PUFAs), or PIP_2 reduction. **(a-b)** Whole-cell voltage clamp recordings of ipRGCs in primary culture showing response to puffer applied OAG (red bar) **(a)** and light stimulus (black bar) during bath application of OAG **(b).** (c-d) Whole-cell recordings of ipRGCs in response to puffer applied arachidonic acid (AA) (red bar) **(c)** and a light stimulus (black bar) during bath application of AA **(d)**. **(e)** Whole-cell recordings of light responses from ipRGCs with control internal solution (black trace) and an ipRGC with wortmannin (red trace) in the internal solution. Both cells were dark adapted for the same period of time. Black bar represents light stimulus. Wortmannin-treated cells, which presumably were slower to replenish PIP_2 in the membrane, showed a dramatic slowing of post-stimulus recovery.

(f,g) Positive control experiments using a heterologously expressed fluorescent biosensor protein in HEK-293 cells (see text) to document the potency of the OAG and AA solutions used in a-d. **(f)** bath application of OAG triggers translocation of the fluorescent PKC-related fusion protein from the cytosol to the plasma membrane. **(g)** Prior incubation with arachidonic acid blocks this OAG-induced movement of PKC into the membrane. Calibration: 50pA and 6s **(a-e)** and 10μm **(g-f)**.